

Figure 3. EMD results obtained by analyzing AE index for both Storm time periods.

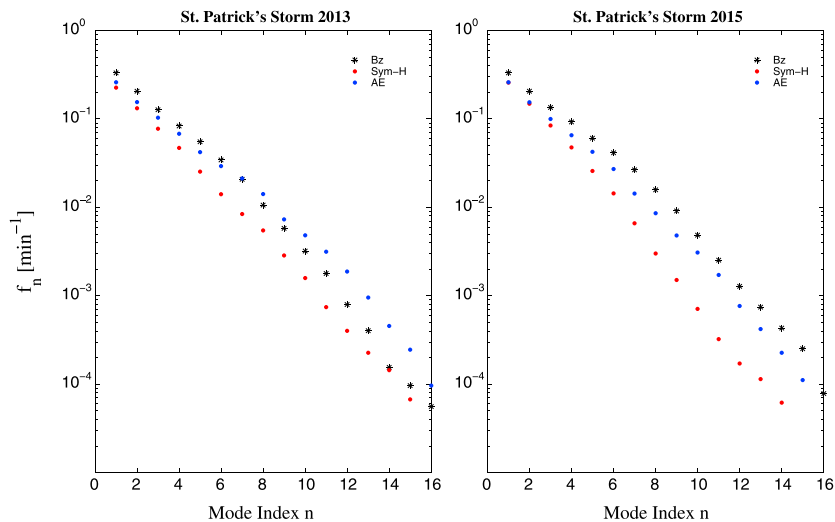


Figure 4. The characteristic frequencies, f_n , versus the mode index, n , for the IMFs relative to B_z (black star), $SYM-H$ (red circles), and AE (blue circles). IMFs for $SYM-H$ and AE are reported in Figures 2 and 3, respectively.

Now although the mutual information $MI(X, Y)$ is able to quantify the statistical independence between two signals/systems, no information is provided in an eventual delay of the interference between the two systems X and Y . A better quantity to address this point is the delayed mutual information $MI(X, Y | \Delta)$ (DMI), which is capable of quantifying a time-dependent statistical independence between the two systems. This quantity is defined as follows:

$$MI(X, Y | \Delta) = \sum_{i,j=1}^N p_{ij}(X(t), Y(t + \Delta)) \log \frac{p_{ij}(X(t), Y(t + \Delta))}{p_i(X)p_j(Y)} \quad (6)$$

where $p_{ij}(X(t), Y(t + \Delta))$ is the joint probability of observing the couple of values (X, Y) , while $p_i(X)$ and $p_j(Y)$ are the probabilities of observing X and Y as independent variables. It can be considered the analog of a cross-correlation function, although it provides an estimation of the total (linear and nonlinear) dependence between two systems/signals [De Michelis et al., 2011] by quantifying the amount of information shared. We underline that the use of DMI to quantify the amount of shared information in the case of SW/IMF parameters and geomagnetic indices is particularly appropriated because of the nonlinear features of the magnetospheric dynamics in response to SW/IMF changes.

To explore the coupling between solar wind (input) and magnetosphere (output) and try to quantify the degree to which one dynamical system affects the dynamics of the other, we use the delayed mutual information $MI(X, Y | \Delta)$.

To quantify the relevance of the dependence/independence degree between two signals using the delayed mutual information $MI(X, Y | \Delta)$, we need to set a significance threshold. This can be done by means of the following procedure. Given two actual time series $\{X_i\}$ and $\{Y_i\}$, an ensemble of $Nr = 10,000$ couples of time series is generated by randomly sorting the two original ones. This operation disrupts any time correlation in each sequence and any possible correspondence between the two time series, without altering the statistics of the values of the actual time series. Hence, for each couple of the randomized time series, we compute the corresponding value of the mutual information $MI(X, Y)$. Then, the statistics of $MI(X, Y)$ values is evaluated by computing the cumulative distribution $C(MI)$. The threshold is chosen at the value MI_{thr} for which $C(MI_{thr}) = 0.95$. This value corresponds to the 5% confidence limit. If the observed value of $MI(X, Y | \Delta)$ is larger than the threshold MI_{thr} , we can say that the observed dependence is significative with an error of 5% at the most.

3. Results and Discussion

We start our analysis of the timescale coupling between solar wind parameters and geomagnetic indices by investigating the scale-to-scale DMI between the IMFs of solar wind parameters and that of geomagnetic indices with similar characteristic frequency.

Figure 5 shows the scale-to-scale DMI in the case of the IMFs relative to the interplanetary magnetic field B_z component and the AE index for the 2013 St. Patrick's Day storm. This analysis clearly evidences how for timescales $\tau < 200$ min the coupling is not significative, while at timescales $\tau \gtrsim 200$ min the coupling becomes significative for time delays Δ in the range $\Delta \in [0, \sim 600-800)$ min. Furthermore, at these large timescales we observe a maximum of the DMI for a delay $\Delta \sim 100$ min, which is consistent with the propagation time of the perturbation from the ACE L1 position to the internal magnetosphere. To avoid any confusion in what follows, we stress that this delay time is not strictly representative of the response time of the Earth's magnetosphere to SW/IMF changes because it also includes the propagation time.

Similar results are found for the scale-to-scale DMI of other quantities (ϵ , $SYM-H$, $AsyH$, AU , and AL) in both the two geomagnetic storms (2013 and 2015 St. Patrick's storms), suggesting that there is a timescale separation in the solar wind-magnetosphere coupling. We observe how this timescale separation occurs at a timescale $\tau \simeq 200$ min, which is in a good agreement with the typical timescale discerning direct driven and loading-unloading magnetospheric processes [Kamide and Kokubun, 1996; Consolini and De Michelis, 2005]. When referring to fluctuations at a certain timescale, the term "direct driven" here is intended according to the linear response theory, i.e., a correspondence between input and output fluctuations at the different timescales unless of a linear filtering.

Moving from this observation of a clear timescale separation for the coupling, we reconstruct two different signals using the EMD. In detail, we divide each set of modes into two subsets: (i) a short-timescale set, with characteristic timescales $\tau \lesssim 200$ min, and (ii) a long-timescale one, with $\tau \gtrsim 200$ min.

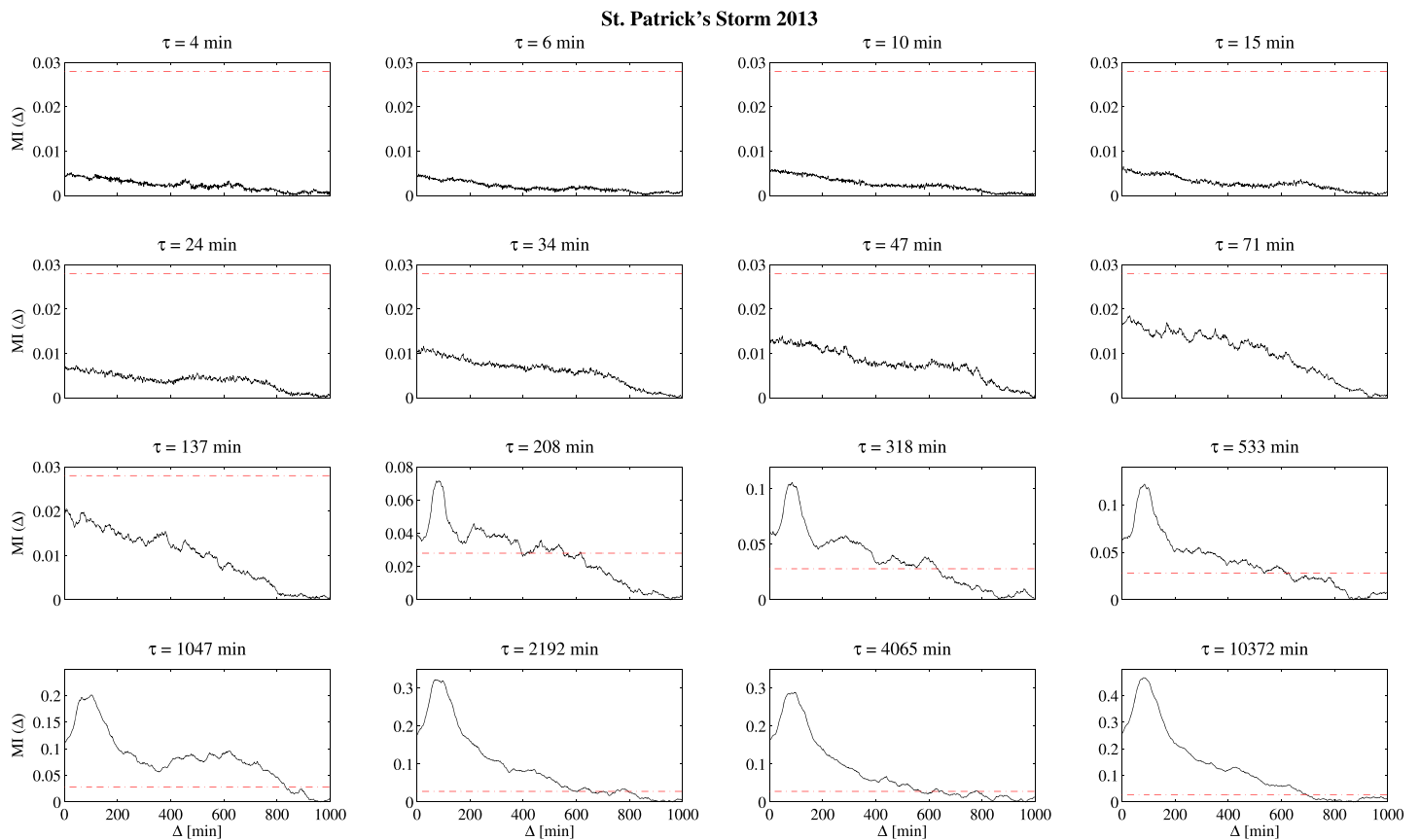


Figure 5. The scale-to-scale DMI between IMFs of the interplanetary magnetic field B_z component and auroral electrojet AE index for the St. Patrick's storm 2013 time period. Red dashed line indicates the significance (5% null hypothesis) DMI threshold, $MI_{thr} = 0.028$.

Figures 6 and 7 show an example of the reconstructed short- and long-timescale signals in comparison with the actual one for the AE index relative to the 2013 St. Patrick's Day storm and the corresponding Fourier spectrum (PSD), respectively. In particular, the PSD clearly shows the relative contribution of the two reconstructed signals to the total PSD of the actual time series, with a frequency cutoff occurring at $f_c \sim 5 \times 10^{-3} \text{ min}^{-1}$. Although the EMD can be thought to act as a low-/high-pass filter, when separating the short- and long-timescale fluctuations, it does not alter the phases of the different spectral contributions, in contrast to standard Fourier-based filters.

The DMI analysis is, then, performed on the reconstructed short- and long-timescale signals relative to the interplanetary magnetic field B_z component and the AE index for the 2013 St. Patrick's Day storm. As shown in Figure 8, a clear and significant amount of shared information (correlation) is found in the case of the long-timescale signals with a maximum of the DMI for a time delay $\Delta \sim 100$ min. Conversely, in the case of short-timescale signals the observed correlation is not significant, indicating that it is reasonable to assume that the processes responsible for the dynamics of Earth's magnetosphere at these timescales are not directly driven by the solar wind parameters. The observed absence of a significant correlation at timescales shorter than 200 min could be due to a *random phase* effect as a consequence of the fact that ACE data have not been adjusted to account for the propagation time between L1 point and the bow shock nose. This random phase effect (acting as a *jitter*) could, indeed, smear out some significant correlation. To check if this hypothesis/interpretation is reasonable, we have attempted two different approaches to correct the results at timescales below 200 min: (i) a OMNI-based propagation method and (ii) a fluid-like based propagation method. Both the two methods (which are discussed in detail in Appendix A) do not produce any significant change in the meaningfulness of the above results (please refer to Appendix A). The main effect of the propagation is the reduction of the time delay Δ in correspondence of which the DMI is maximal. In particular, we get a maximum of the DMI for a time delay of $\Delta \sim 50\text{--}70$ min. Furthermore, conversely to what is expected, the meaningfulness of DMI at timescales shorter than 200 min does not show any significant change, as it is

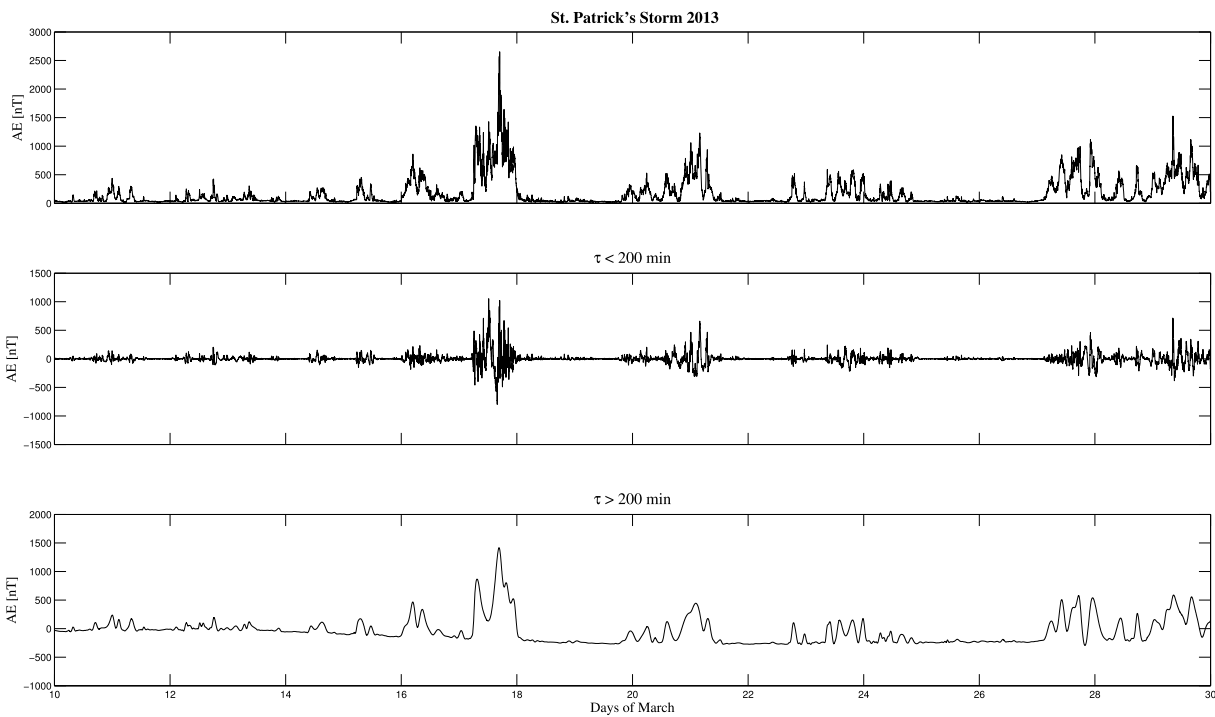


Figure 6. (top) The actual, (middle) the short-timescale ($\tau < 200$ min), and (bottom) the long-timescale ($\tau > 200$ min) signals of AE index for the St. Patrick's storm 2013 time period.

for the timescales longer than 200 min. These results suggest that the Earth's magnetospheric dynamics play a very relevant role at timescales shorter than 200 min, confirming what has been extensively documented in several previous works [Tsurutani et al., 1990; Kamide and Kokubun, 1996; Consolini, 1997; Sitnov et al., 2001; Uritsky et al., 2002; Consolini and De Michelis, 2005].

To better investigate this point we extend the above analysis to all the other parameters considered in this work and also for the St. Patrick's Day storm that occurred in 2015.

Figure 9 shows the results of the DMI analysis for the actual and reconstructed time series in the case of SYM-H, ASY-H, AU, and AL versus IMF B_z component, and SYM-H, ASY-H, AE, AU, and AL versus the Perrault-Akasofu coupling function ϵ . All the cases confirm the previous results. Timescales longer than 200 min are directly

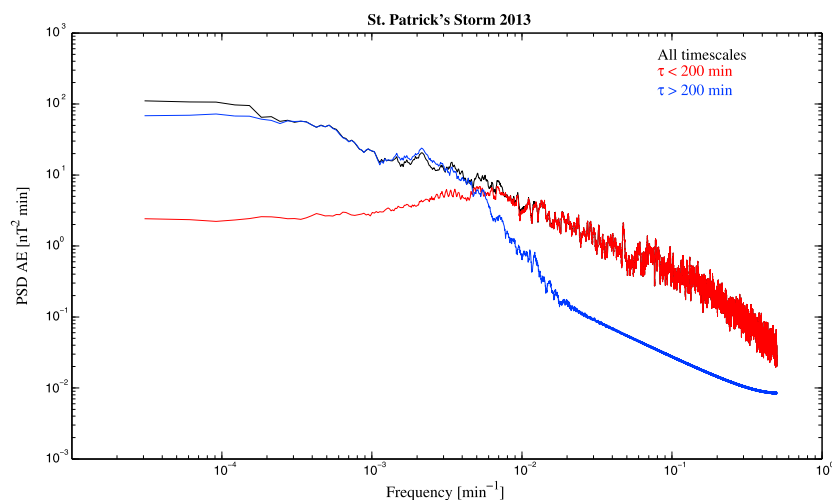


Figure 7. The PSD of the actual and reconstructed signals of AE index for the St. Patrick's storm 2013 time period. Black, red, and blue lines refer to actual, short-timescale ($\tau < 200$ min), and long-timescale ($\tau > 200$ min) signals, respectively.